ChemCatChem

Research Article
doi.org/10.1002/cctc.202300811

Chemistry Europe
European Chemical Societies Publishing

www.chemcatchem.org

Pt Nanoparticles on Beta zeolites for Catalytic Toluene Oxidation: Effect of the Hydroxyl Groups of Beta Zeolite

Run Zou,[a, b] Sarayute Chansai,[a] Shaojun Xu,[a] Bing An,[c] Shima Zainal,[a] Yangtao Zhou,[b] Ruojia Xin,[a] Pan Gao,[d] Guangjin Hou,[d] Carmine D'Agostino,[a] Stuart M. Holmes,[a] Christopher Hardacre,*[a] Yilai Jiao,*[b] and Xiaolei Fan*[a]

Stabilisation of metal species using hydroxyl-rich dealuminated zeolites is a promising method for catalysis. However, insights into the interactions between the hydroxyl groups in zeolite and noble metals and their effects on catalysis are not yet fully understood. Herein, comparative studies were conducted using Pt catalysts supported on hydroxyl-rich dealuminated Beta (deAl-Beta) and the pristine proton-form Beta (H-Beta) for catalytic oxidation of toluene. The findings suggest that during impregnation the Pt precursor (i.e., $Pt(NH_3)_4(NO_3)_2$) interacted with different sites on deAl-Beta and H-Beta, leading to the formation of supported Pt nanoparticles with different physicochemical properties. In detail, for H-Beta, the Pt precursor interacted with Al-OH and isolated external Si-OH sites, yielding Pt NPs with a higher Pt^0 proportion of ~71% compared to ~57% Pt^0 on deAl-Beta. Comparatively, abundant hydroxyl groups on deAl-Beta such as silanol nest and isolated internal Si-OH stabilised highly active Pt-O species. The resulting Pt/deAl-Beta exhibited improved activity and anti-coking ability than Pt/H-Beta in catalytic toluene oxidation. For example, the temperature for 50% toluene conversion was 193 °C for Pt/deAl-Beta vs. 232 °C for Pt/H-Beta, and the coke deposition was 1.7% vs. 6.7% (after the 24-h longevity test), respectively. According to the toluene-temperature programmed desorption (toluene-TPD), ^{1}H nuclear magnetic resonance (^{1}H NMR) relaxation and *in situ* diffuse reflection Fourier transform spectroscopy (in situ DRIFTS) characterisation, the enhanced performance of Pt/deAl-Beta could be ascribed to (i) the active Pt-O sites stabilised by hydroxyl groups, which interact with toluene easily for conversion, and (ii) the acid-free feature of the deAl-Beta support, which avoids the formation of coke precursors (such as benzoate species) on the catalyst surface. Findings of the work can serve as the design guidelines for making effective supported metal catalysts using zeolitic carriers.

Introduction

Volatile organic compounds (VOCs) are dangerous to human health and environment. Accordingly, many technologies are designed and employed for VOC recovery and destruction, such as adsorption, membrane separation, thermal degradation and catalytic oxidation.[1,2] Among these solutions, catalytic oxidation is considered to be one of the effective technologies for VOC degradation because it can convert VOCs to CO_2 and H_2O with higher destructive efficiency and without by-products formation under relatively mild conditions, as well as being able to be applied to dilute VOC streams. Toluene is a typical aromatic VOC, which is considered as a prior pollutant due to its moderate toxicity even at low concentrations (e.g.,

[a] R. Zou, S. Chansai, S. Xu, S. Zainal, R. Xin, C. D'Agostino, S. M. Holmes, C. Hardacre, Dr. X. Fan
Department of Chemical Engineering
School of Engineering
The University of Manchester
Oxford Road
Manchester, M13 9PL (UK)
E-mail: c.hardacre@manchester.ac.uk
xiaolei.fan@manchester.ac.uk

[b] R. Zou, Y. Zhou, Y. Jiao
Shenyang National Laboratory for Materials Science
Institute of Metal Research
Chinese Academy of Sciences
72 Wenhua Road
Shenyang, 110016 (P. R. China)
E-mail: yljiao@imr.ac.cn

[c] B. An
Department of Chemistry
School of Sciences
The University of Manchester
Oxford Road
Manchester, M13 9PL (UK)

[d] P. Gao, G. Hou
State Key Laboratory of Catalysis
National Laboratory for Clean Energy
2011-Collaborative Innovation Center of Chemistry for Energy Materials
Dalian Institute of Chemical Physics
Chinese Academy of Sciences
Zhongshan Road 457
Dalian 116023 (P. R. China)

[**] A previous version of this manuscript has been deposited on a preprint server (https://doi.org/10.1016/j.mcat.2023.112951).

Supporting information for this article is available on the WWW under https://doi.org/10.1002/cctc.202300811

<100 ppm).[3] To date, various types of catalysts have been developed for catalytic oxidation of toluene, mainly including the transition metal oxides and noble metal-based catalysts.[4] Compared to transition metal oxides, the noble metal-based catalysts, represented by the platinum family metals, have been widely studied and applied due to the high intrinsic activity.[5] To promote the performance of Pt-based catalysts, different support materials have been explored to modulate the properties of the supported Pt species (e.g., better dispersion and/or more Pt^0 species) such as Al_2O_3,[6] silica,[7] CeO_2[8] and zeolites.[9] Among them, zeolites have been identified as good candidates due to their relatively high surface area, ion-exchange ability and good thermal stability, as well as the structural flexibility to regulate the metal species (such as the hierarchical zeolites[10–14]). For example, the hierarchical ZSM-5 with the micro-meso-porous structure could improve the dispersion of Pt species, and thus enhance the toluene oxidation performance.[10] Additionally, by exchanging the charge-compensating cations in proton-form Beta zeolite to alkali ions (e.g., Na^+ and K^+), the resulting supported Pt catalysts showed better toluene oxidation performance due to the formation of more Pt^0 species.[15] Recent studies also shows that the modification of zeolite by demetallation (e.g., dealumination) can tune the acidity and surface properties (e.g., surface hydroxyl groups and hydrophobicity), which have considerable effects on the supported metal nanoparticles (NPs) and adsorption/desorption of reactant/product in catalysis.[16,17]

Dealumination is a common post-synthetic approach to remove Al species from zeolitic frameworks to create hydroxyl groups such as silanol nest (T-site defect),[18,19] which enables the stabilisation of metal species and modulation of their properties. This is exemplified by the formation of highly-dispersed metal species (e.g., Co,[20] V,[21] Cu[22] and Ni[23]) in dealuminated Beta zeolite (deAl-Beta). For example, Dzwigaj et al.[23] reported the preparation of small Ni nanoparticles (~7 nm, with Ni loading of 10 wt.%) supported on deAl-Beta for CO_2 methanation. Comparing to catalyst supported by H-Beta, the Ni/deAl-Beta catalyst showed better CO_2 conversion and CH_4 selectivity at relatively low temperatures (250–350 °C) due to the high Ni dispersion. In addition, the silanol nest can also facilitate the formation of unique metal oxides or bimetallic alloys.[24,25] For example, highly-active supported ZnO_x species (for propane dehydrogenation) can be formed by reacting the Zn^0 species with silanol nest in deAl-Beta (via *in situ* reduction of ZnO_x), leading to three times higher propene productivity at similar propene selectivity than the commercial K-CrO_x/Al_2O_3.[24] The silanol nests in the mesoporous MFI zeolite (after removal of gallium, deGa) could activate the hard-to-reduce rare-earth elements (e.g., La and Y with low reduction potential) effectively by arranging them as single atomic species to overcome the energy hurdle, which facilitates the formation of alloy NPs.[25]

Recent studies also demonstrated the successful development of supported metal catalysts on deAl-Beta for catalytic oxidation of toluene including monometallic CoO_x/deAl-Beta[26] and bimetallic $CuMnO_x$/deAl-Beta,[27] in which a homogeneous distribution of the active phases over the support was achieved. For example, highly dispersed isolated mononuclear Co(II) species, small Co(II) oxide clusters and/or Co_3O_4 crystallites were incorporated into the framework of Beta zeolite by changing the amount of the introduced Co from 3 to 9 wt.%.[26] The resulting CoO_x/deAl-Beta with higher Co loading showed higher toluene oxidation activity due to the formation of more active Co_3O_4 phase. However, it is worth noting that, compared to the catalyst supported by H-Beta (i.e., CoO_x/H-Beta), the CoO_x/deAl-Beta catalyst showed very similar conversion of toluene and yield of CO_2 and CO. Similarly, highly dispersed bimetallic $CuMnO_x$ phases were supported on deAl-Beta as well by varying the Cu/Mn ratio during impregnation.[27] The mixed oxides catalysts with increased surface oxygen vacancies showed a better catalytic performance than the monometallic catalysts (i.e., Cu/deAl-Beta and Mn/deAl-Beta). However, the comparison of performances between catalysts supported by H-Beta and deAl-beta was not discussed. Hence, previous studies on the transition metal-based catalysts showed the advantages deAl-Beta as the catalyst carrier to improve catalytic oxidation reactions. In light of the importance of Pt-based catalysts in VOCs oxidation catalysis, insights into the metal-support interactions for the catalysts based on deAl-Beta, and their effects on the oxidation performances are not yet understood.

Herein, comparative studies were carried out to investigate the effect of hydroxyl groups in Beta zeolite on the physicochemical properties of the supported Pt species and their activity in catalytic toluene oxidation. In detail, the supported Pt on H-Beta and deAl-Beta zeolite catalysts were prepared by impregnation, and the resulting catalysts, denoted Pt/deAl-Beta and Pt/H-Beta, respectively, were fully characterised (regarding particle size, metal dispersion, oxidation state, electronic and coordination structure of the supported Pt NPs) to elucidate the effect of hydroxyl groups on the properties of the supported Pt NPs. The interactions between the Pt precursor (i.e., Pt-$(NH_3)_4(NO_3)_2$) and zeolite supports (which is reflected by the variation of the surface hydroxyl groups in the catalysts during synthesis and work-up) were probed by solid state ^{1}H nuclear magnetic resonance (*ss*-^{1}H NMR) and *in situ* diffuse reflection Fourier transform spectroscopy (in situ DRIFTS). The catalytic performance of the two catalysts was assessed by catalytic oxidation of toluene. Further characterisations of the catalysts and catalytic systems were conducted using toluene-temperature programmed desorption (toluene-TPD), ^{1}H NMR relaxation and *in situ* DRIFTS characterisation to gain mechanistic insights into the difference in the measured activities and coke formation.

Results and Discussion

Physicochemical properties of Pt/deAl-Beta and Pt/H-Beta

The H-Beta and deAl-Beta were characterized by various techniques, and the relevant results (Figure S1 and S2) show that the morphology (by TEM, Figure S1), textural (by N_2 physisorption, Figure S2 and Table S1), and crystalline (Figure 1) properties of deAl-Beta were retained after dealumination

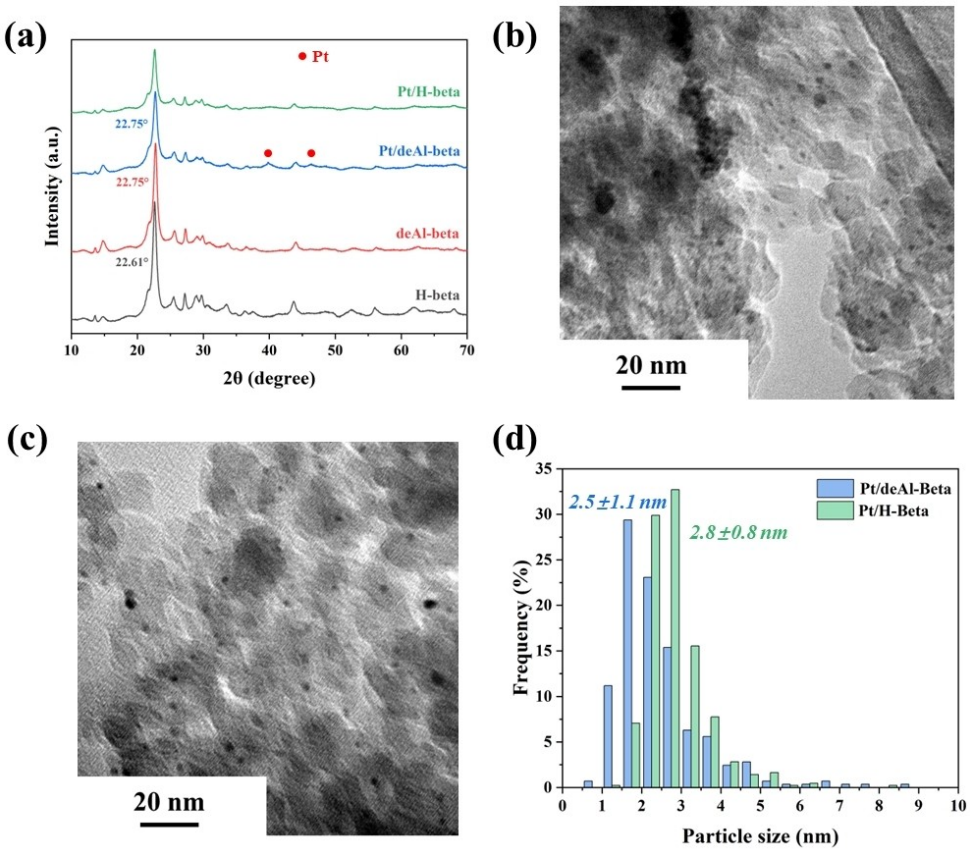

Figure 1. Physical properties of the zeolite supports and the Pt catalysts under investigation: (a) XRD patterns, (b–d) HRTEM micrographs of (b) Pt/deAl-Beta and (c) Pt/H-Beta, and (d) particle size distribution of the two catalysts (based on statistics of counting ca. 400 particles from relevant HRTEM images).

(compared to H-Beta), whilst the acidity of deAl-Beta was reduced significantly (by NH_3-TPD, Figure S3, SAR of deAl-Beta was estimated as >1000 by ICP). XRD patterns (Figure 1a) show that the reduced Pt/deAl-Beta exhibits distinct diffraction peaks of Pt (111) and (200) facets at 2θ of 39.8° and 46.3° (JCPDS NO. 04–0802), respectively, suggesting the presence of Pt crystalline in Pt/deAl-Beta. Conversely, the diffraction peaks of the Pt phase were less obvious in the reduced Pt/H-Beta. HRTEM micrographs (Figure 1b and 1c), and the particle size distribution (<10 nm, Figure 1d) show that the size of small Pt NPs on Pt/deAl-Beta and Pt/H-Beta is 2.5 ± 1.1 nm and 2.8 ± 0.8 nm, respectively, and the former has more NPs with sizes smaller than 2 nm. HAADF-STEM analysis (Figure S4) showed Pt particle agglomeration on both catalysts, which could be associated to the incomplete impregnation of the metal precursor on the supports.[28] N_2 physisorption (Figure S2, Table S1) shows that deAl-Beta displays slightly higher porosity (specific surface area, $S_{BET}=581$ m^2/g) than H-Beta ($S_{BET}=516$ m^2/g). After Pt loading, a decrease in porosity was observed for Pt/deAl-Beta. The S_{BET} was 581 m^2/g for deAl-Beta vs. 395 m^2/g for Pt/deAl-Beta, and the specific micropore area, S_{micro}, was 360 m^2/g for deAl-Beta vs. 266 m^2/g for Pt/deAl-Beta. The considerable reduction in microporosity/mesoporosity in Pt/deAl-Beta might be due to the pore blockage by Pt NPs interacting strongly with the dealuminated zeolite framework[23] and/or locating at the intercrystalline voids (as the Beta zeolite is in the form of nanocrystals, Figure S1). Conversely, the Pt/H-Beta showed almost preserved porosity ($S_{BET}=513$ m^2/g) in comparison with the bare H-Beta support ($S_{BET}=516$ m^2/g).

The chemical properties of the Pt catalysts were studied by H_2-TPR, XPS, CO-DRIFTS and XAFS. H_2-TPR (Figure 2a) reveals that Pt/deAl-Beta displays two intense reduction peaks at about 193 °C and 431 °C. The peak at the lower temperature could be assigned to the reduction of Pt^{2+} species on external surface with a relatively weak interaction,[29] whilst the peak at ~431 °C could be correlated to the Pt species interacting strongly with the framework of deAl-Beta. In contrast, Pt/H-Beta can be reduced at relatively lower temperatures with reduction peaks at 211 and 349 °C indicating relatively weak interactions between Pt species and H-Beta. The oxidation state of the reduced Pt catalysts was studied by XPS (Figure 2b). Deconvolution of Pt $4f_{7/2}$ spectra shows two peaks at the binding energy (B.E.) of 71.5 and 73.0 eV, corresponding to the Pt^0 and Pt^{2+} species, respectively. Specifically, Pt/H-Beta exhibits higher surface Pt metallic state (Pt^0 ~71 %) than Pt/deAl-Beta (Pt^0~57 %), which is consistent with the H_2-TPR results above. Note that the Al 2p peak envelope was not considered in the XPS fitting of Pt/deAl-Beta since it is very insignificant.

It is speculated that the higher oxidation state of Pt in Pt/deAl-Beta is due to the Pt-hydroxyl groups interaction, leading

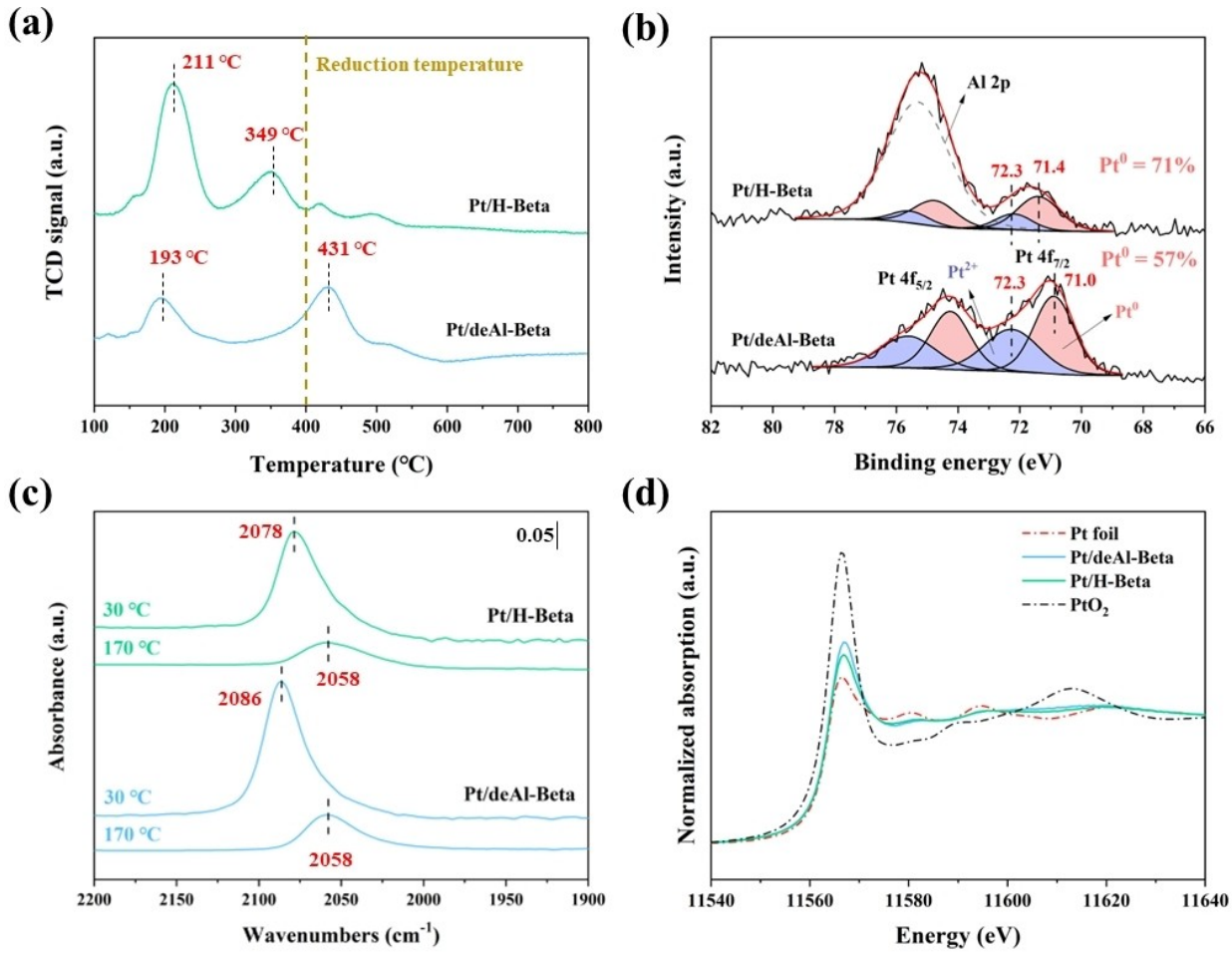

Figure 2. Chemical properties of the Pt catalysts probed by (a) H_2-TPR, (b) XPS, (c) CO-DRIFTS (CO adsorption at 30 and 170 °C with subsequent Ar purging to remove the CO in gas phase) and (d) XANES.

to the formation of oxidized Pt species being difficult to be reduced. CO-DRIFTS spectra of the Pt catalysts at 30 and 170 °C (after argon purging, Figure 2c) show a broad CO adsorption band 2100–2000 cm^{-1}, which can be assigned to the linear adsorption of CO on Pt surface.[30] At 30 °C, Pt/H-Beta showed a CO adsorption band at a lower wavenumber (2078 cm^{-1}) in comparison with that of Pt/deAl-Beta (at 2086 cm^{-1}), which is consistent with the presence of more reduced Pt phases in Pt/H-Beta.[31] It is worth noting that at both 30 °C and 170 °C the CO adsorption band intensity of Pt/deAl-Beta is stronger than that of Pt/H-Beta, indicating the presence of more accessible Pt surface in Pt/deAl-Beta. To obtain detailed structural information of Pt species, XANES and EXAFS characterisations were conducted. The Pt L_3-edge XANES spectra (Figure 2d) show that the white line of the two Pt catalysts were between the Pt foil and PtO_2, indicating a mixed Pt valent state of Pt^0 and Pt^{2+}. Specifically, Pt/deAl-Beta showed an increased intensity of the white line than Pt/H-Beta, confirming that it possesses Pt species with higher oxidation state and smaller sizes. These results were also confirmed by EXAFS analysis (Figure S5, Table S2). The average coordination number (CN) of Pt-O and Pt-Pt bond in Pt/deAl-Beta is 2.10 ± 0.58 and 5.28 ± 1.86, whilst in Pt/H-Beta the CNs were 1.98 ± 0.05 and 7.04 ± 1.83, respectively. Therefore, the results above suggest that deAl-Beta is able to stabilize oxidised Pt species via the stronger guest-host interaction involving Pt-O bonds in its framework, possibly via the hydroxyl groups resulted from dealumination.

Evolution of hydroxyl groups during catalyst preparation

To gain insights into the interactions between the Pt precursor and the two Beta supports during synthesis, *ss*-^{1}H NMR and *in situ* DRIFTS were applied to reveal the changes of hydroxyl groups during and/or after the reduction of the Pt catalysts. ^{1}H NMR spectra are shown in Figure 3a (peak fitting results were presented in Table S3, note that the peak areas were normalised by the intensity of the isolated external Si-OH in H-Beta for comparison), the bare H-Beta presents four different hydroxyl groups including Al-OH (~0.7 and 2.8 ppm), isolated external Si-OH (~1.8 ppm), silanol nest (~2.0 ppm) and bridging Si-OH-Al (~4.1 ppm, the Brønsted acid site).[32] Dealumination of H-Beta caused (i) the elimination of Al-OH and Brønsted acid site and reduction of isolated external Si-OH (which is reflected by the

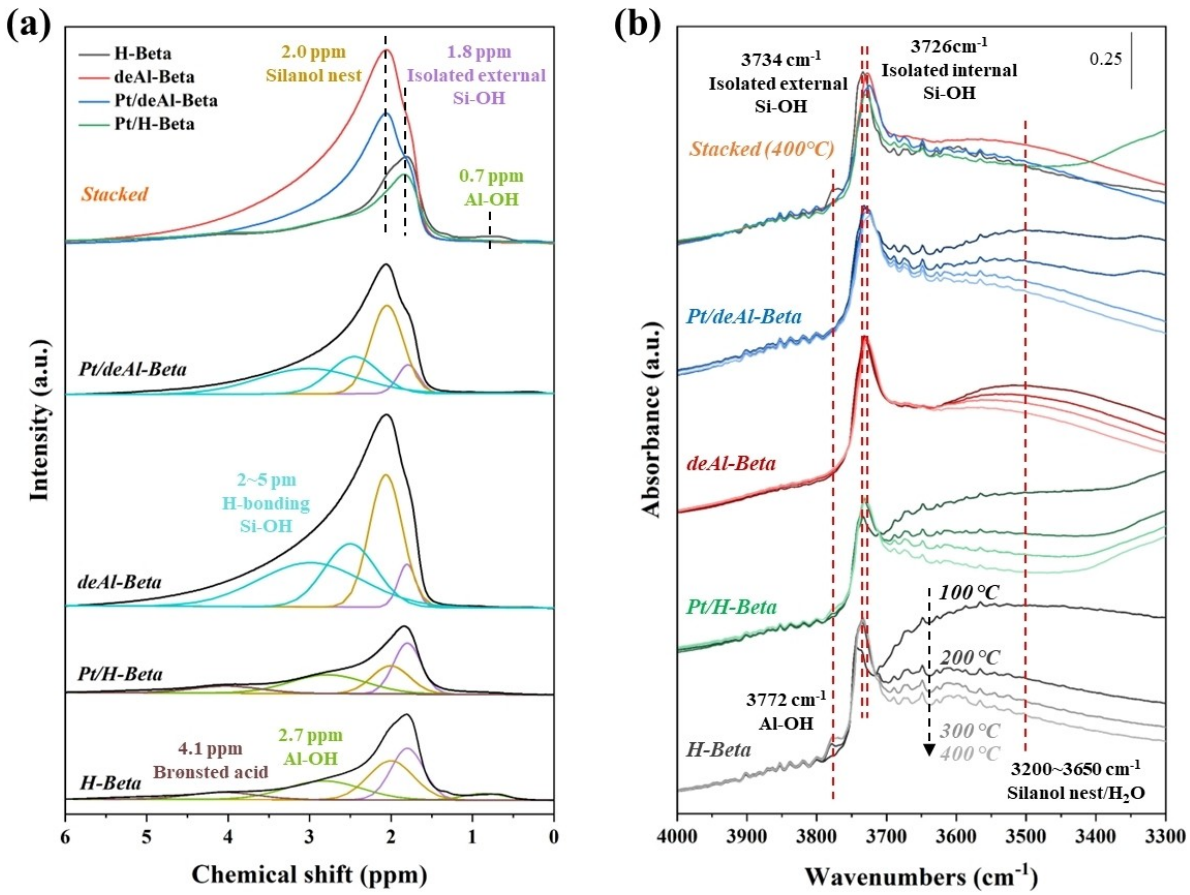

Figure 3. (a) *ss*-^{1}H NMR spectra of the two Beta zeolite supports and relevant Pt catalysts; (b) evolution of hydroxyl groups in the Beta zeolites and the Pt catalysts during thermal reduction (with 5 vol.% Ar-balanced H_2 at 60 mL/min) probed by *in situ* DRIFTS.

decrease in intensity from 1.00 to 0.45), (ii) the significant formation of silanol nest at ~2.0 ppm in deAl-Beta (intensity increased from 1.05 to 2.58), and (iii) the emergence of the H-bonded Si-OH groups (i.e., the broad peak at 2–5 ppm with the intensity of 4.66).[33] Notably, after Pt loading, the peak of Al-OH in Pt/H-Beta (at ~0.7 ppm) disappeared completely (with initial intensity of 0.16), and the isolated external Si-OH and silanol nest decreased (from 1.00 to 0.83 and 1.05 to 0.63, respectively). The results agree with findings reported previously, wherein, the Pt precursor (e.g., $Pt(NH_3)_4(NO_3)_2$) could interact with the extraframework Al species (EFAL) and isolated external Si-OH in H-Beta.[34] Regarding deAl-Beta, after Pt loading the band intensity of the silanol nest, H-bonded Si-OH and isolated external Si-OH decreased (Table S3). In summary, for the H-Beta support, the Pt loading caused 100% reduction for Al-OH, 17% reduction for isolated external Si-OH and 40% reduction for silanol nest. Conversely, for the deAl-Beta support, site reduction for isolated external Si-OH, H-bonded Si-OH and silanol nest is 20%, 45% and 34%, respectively. The results suggest that during Pt impregnation, the Pt precursor tends to interact with the Al-OH site and silanol nest in H-Beta. After dealumination, the silanol nest and H-bonded Si-OH sites are the primary sites for binding the Pt precursor.

In situ DRIFTS characterisation was conducted to reveal the dynamics of hydroxyl groups of the two supports and relevant Pt catalysts during hydrogen reduction (from 100 to 400 °C, at 10 °C/min). As shown in Figure 3b, at 100 °C the OH-stretching absorbance of the adsorbed water in H-Beta and Pt/H-Beta was observed at 3200–3700 cm^{-1}, and a significant decrease in the intensity of the broad band was measured *in situ* by increasing the reduction temperature (especially at $<$200 °C, due to the removal of physically adsorbed water). The band at about 3772 cm^{-1} can be assigned to Al-OH in H-Beta,[32] and it was absent at 100 °C initially and emerged gradually with an increase in treatment temperature due to water desorption from the hydrophilic Al-OH. Interestingly, in Pt/H-Beta the Al-OH was absent during the entire reduction treatment, suggesting that the Pt-(Al-OH) interaction occurred during impregnation synthesis. Due to dealumination, the Al-OH band was not identified and that associated with water adsorption was less intense in the spectra of deAl-Beta and Pt/deAl-Beta during the *in situ* DRIFTS characterisation. The broad band in the DRIFTS spectra of deAl-Beta and Pt/deAl-Beta at around 3500 cm^{-1} can be assigned to silanol nest,[28] and the associated band intensity decreased by increasing the treatment temperature due to its condensation[29] and/or interaction with Pt species (according to the findings above by *ss*-^{1}H NMR). Moreover, the stacked spectra at 400 °C also indicate the consumption of Al-OH and isolated external Si-OH in Pt/H-Beta, whilst the band intensity of the isolated internal Si-OH and silanol nest decreased in Pt/

deAl-Beta, being in line with the findings by *ss*-^{1}H NMR. Therefore, the results above confirm that on deAl-Beta the abundant hydroxyl groups (especially silanol nest and H-bonded Si-OH sites) are prone to interact with the Pt precursor, contributing to the strong guest-host interaction *via* Pt-O bonds in the Pt/deAl-Beta catalyst.

Catalytic performance of the Pt catalysts

Catalytic oxidation of toluene over the Pt catalysts under investigation was conducted to study the structure-performance relationship. To avoid negative toluene conversion due to toluene desorption at elevated temperature from the catalysts (Figure S6), the MS signal of CO_2 was used to plot the light-off characteristic of the catalysts. Higher Pt dispersions and/or more Pt^0 species are expected to favour catalytic oxidation reactions.[35] Interestingly, the comparative catalytic results show that Pt/deAl-Beta exhibited the best activity among the catalysts under investigation, with the lowest temperature for 50% conversion of toluene (T_{50}) of 193 °C (Figure 4a). In contrast, Pt/H-Beta presented the worst catalytic performance with T_{50} of 232 °C. The bare H-Beta and deAl-Beta supports exhibit poor performance in the oxidation reaction (Figure S7). The abundant hydroxyl groups in deAl-Beta and their interactions with the Pt species seem important to the activity of Pt/deAl-Beta in catalytic toluene oxidation. To support this, a control catalyst based on calcinated deAl-Beta (which possesses less hydroxyl groups compared to the as-prepared deAl-Beta) was prepared (i.e., Pt/calcinated deAl-Beta, relevant characterisations of the control were shown in Figure S8) and assessed, showing a lower activity (with T_{50} = 206 °C) than Pt/deAl-Beta. Interestingly, although the control catalyst of Pt/H-Beta 150 showed severe Pt agglomeration (with the Pt NPs sizes of ~19.1 ± 6.8 nm, detailed physiochemical characterisations were shown in Figure S9), it still outperformed Pt/H-Beta (T_{50}: 213 °C vs. 232 °C), which could be due to the less acidity in H-Beta 150 compared to H-Beta. The results suggest that in addition to nature of the supported Pt species, the property of the Beta zeolite carriers (such as acidity) was important as well on affecting the catalytic oxidation activity. Pt/H-Beta and Pt/deAl-Beta were selected for the longevity tests (in presence of 4.5 vol.% water), and the results show no obvious deactivation during the 24 h on stream (Figure S10). Notably, TGA of the used catalysts after the longevity test (Figure S11) suggests less coke formation on Pt/deAl-Beta (~1.7 wt.%) than Pt/H-Beta (~6.7 wt.%), which could be due to the absence of acidity in Pt/deAl-Beta. Hence, the improved activity and anti-coking ability of Pt/deAl-Beta could be related to the stabilised Pt species (by the hydroxyl groups) and absence of acidity on/from the deAl-Beta zeolite support. To further understand the guest-host interactions in the catalysts and associated catalytic systems, toluene-TPD and ^{1}H NMR relaxation measurements of the catalysts were performed.

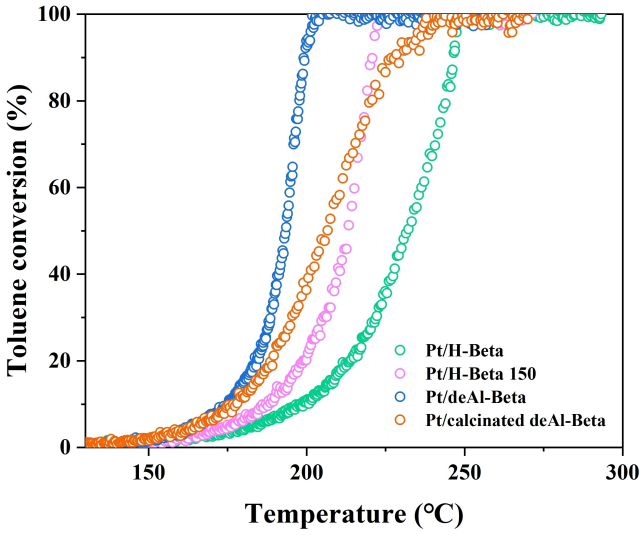

Figure 4. Light-off curves of the Pt catalysts under investigation in catalytic oxidation of toluene (0.05 g catalyst, 500 ppm toluene + 20 vol.% O_2 + Ar with total flow rate of 160 mL/min).

Interactions between toluene and the zeolites/catalysts

Toluene-TPD was performed to gain information on the interaction between the reactant molecule with the zeolite supports and Pt catalysts. Figure 5a shows that the interaction strength between toluene and the zeolite supports/catalysts is different, which is reflected by the higher temperature for full desorption (T_{com}) of H-Beta and Pt/H-Beta than deAl-Beta and Pt/deAl-Beta (~249 vs. ~210 °C), suggesting that it contains adsorption sites to bind toluene strongly (likely the acid site[36]). The toluene desorption peak temperature (T_{peak}) of Pt/H-Beta is higher than that of Pt/deAl-Beta, indicating the presence of Pt sites bound strongly with toluene as well. The desorption peak area was normalised using the specific surface area of the supports/catalysts to estimate the specific adsorption amount. The toluene adsorption capacity of deAl-Beta (1.06×10^{-3} mmol/m^2) is higher than that of H-Beta (0.99×10^{-3} mmol/m^2), possibly due to the increased interactions induced by the abundant hydroxyl groups in deAl-Beta. Notably, after Pt loading, the toluene adsorption capacity of Pt/deAl-Beta increased by about 20% in comparison with that of deAl-Beta, showing that the Pt species in Pt/deAl-Beta tended to interact with toluene. Conversely, the toluene adsorption capacity of Pt/H-Beta (0.94×10^{-3} mmol/m^2) is slightly lower than that of H-Beta (0.99×10^{-3} mmol/m^2).

The guest-host interaction in the supports/catalysts was further probed by NMR relaxation. Figure 5b presents the ratio of the spin-lattice to spin-spin relaxation time constant (T_1/T_2, which is an indicator of the affinity of guest molecules with the solid surface and has been recently validated in zeolites[37–39]) of toluene within the supports/catalysts under investigation. The calculated T_1/T_2 values of deAl-Beta and Pt/deAl-Beta are much higher than that of H-Beta and Pt/H-Beta, confirming the stronger interaction between toluene molecules and the surface of deAl-Beta. In addition, the Pt loading on deAl-Beta resulted in a considerable increase in the T_1/T_2 ratio, i.e., 35 for deAl-Beta

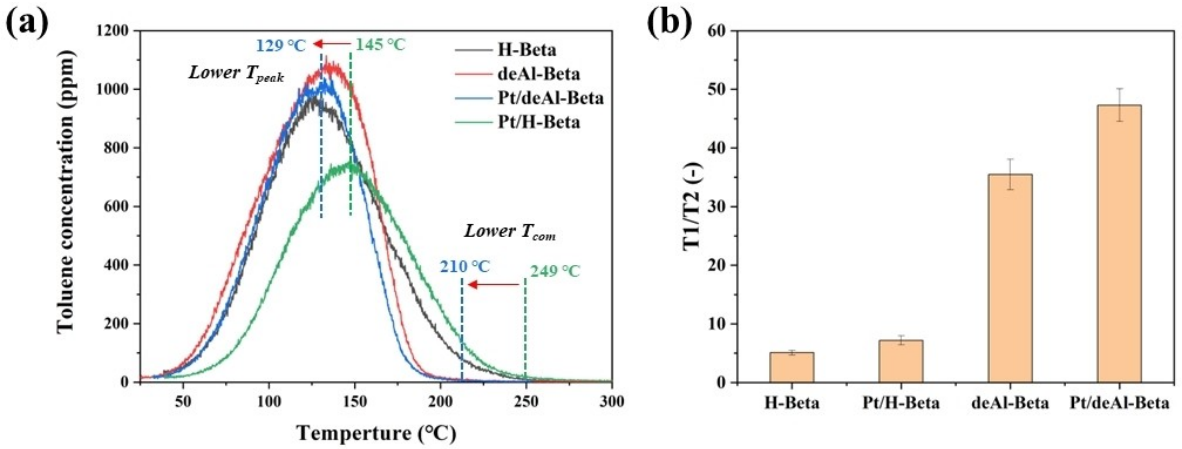

Figure 5. Toluene interaction with the Beta zeolite supports and the supported Pt catalysts by (a) toluene-TPD and (b) NMR relaxation measurements.

vs. 47 for Pt/deAl-Beta (comparatively, 5 for H-Beta vs. 7 for Pt/H-Beta), suggesting the strong ability of Pt/deAl-Beta to interact with toluene. The results of NMR relaxation are consistent with the findings of toluene-TPD. In combination with the catalytic data, it is possible to infer that the better catalytic performance of Pt/deAl-Beta could be related to its strong ability to interact, and subsequently activate, toluene molecules.

In situ DRIFTS studies

To understand the guest-host interactions under relevant reaction conditions, *in situ* DRIFTS characterisation were conducted for the two Pt catalysts (Figure 6). As shown in Figure 6a and 6b, with toluene and O_2 at 50 °C, on Pt/deAl-Beta (which was reduced *in situ* at 400 °C), the intensity of relevant bands (i.e., C–H stretching vibration of the aromatic ring at 3085, 3059 and 3029 cm^{-1}, C–H symmetric and asymmetric stretching vibration of methyl group at 2922 and 2872 cm^{-1} and C–C skeletal vibration of the benzene ring at 1602 and 1493 cm^{-1})[40] is significantly higher than that on Pt/H-Beta, proving the stronger interaction between Pt/deAl-Beta and toluene, and confirming the results of toluene-TPD and NMR relaxation. Notably, the negative adsorption bands at 3732 cm^{-1} (isolated internal Si-OH) and/or 3781 cm^{-1} (Al-OH) together with the positive band at 3596 cm^{-1} in two Pt catalyst indicate the presence of interactions between the methyl group of toluene and the relevant hydroxyl groups in the catalysts.[41,42] Specifically, the stronger band intensity at 3596 cm^{-1} and 3732 cm^{-1} in Pt/deAl-Beta relevant to that in Pt/H-Beta indicates that the isolated internal Si-OH could promote toluene adsorption. In addition, the adsorption bands at 1298, 1463 and 1169 cm^{-1} could be assigned to the CH_2 deformation vibration (1298 cm^{-1}) and C–O stretching vibration (1463 and 1169 cm^{-1}), respectively, indicating the presence of surface benzyl alcohol.[41–44] For comparison, the DRIFTS spectrum of toluene adsorption on Pt/calcinated deAl-Beta (with less hydroxyl groups) at 170 °C shows no band at 1169 cm^{-1} (Figure S8f). Hence, the DRIFTS results suggest that hydroxyl groups in deAl-Beta enabled chemisorption of toluene.

With an increase in temperature (from 50 to 210 °C, at 10 °C/min), the intensity of relevant adsorption bands above (i.e., toluene and benzyl alcohol) decreased gradually in both Pt catalysts, indicating the consumption of surface species due to catalytic oxidation. Interestingly, on Pt/deAl-Beta (Figure 6a), new adsorption bands at 1701 (CO stretching vibration of benzaldehyde),[41,45,46] 1844 and 1775 (C–O stretching vibrations of maleic anhydride)[46–50] and 1525 cm^{-1} (antisymmetric C–O stretching vibration of benzoate)[47,51] appeared, corresponding to the intermediates of toluene oxidation. In contrast, as shown in Figure 6b, two significant bands at 1525 and 1584 cm^{-1} developed gradually on Pt/H-Beta relating to the skeletal C–C stretching vibrations of benzoate.[46,49] Such surface species on Pt/H-Beta could be the precursors for coking,[51] which was evidenced by TPO studies of the used catalysts (from the longevity tests). CO_2 formation was observed at ca. 200 and 515 °C from the used Pt/H-Beta catalyst (Figure S12), which could be assigned to oxygenated aromatic compounds and bulky polyaromatic compounds, respectively.[52] The significant coke formation in Pt/H-Beta could be related to the Brønsted acidity of H-Beta,[49] and was likely on the Pt surface and/or deposited in the pores of the zeolite support as no visible bulky carbonaceous species can be observed in the TEM micrograph, Figure S12b).

Time-resolved *in situ* DRIFTS of toluene oxidation was further conducted for the two Pt catalysts at constant temperatures (i.e., at 170 °C for Pt/deAl-Beta and 200 °C for Pt/H-Beta, respectively, to achieve the comparable conversions of about 10%, Figure 6c). The reaction feed (i.e., Ar-balanced toluene + O_2) was introduced to the catalysts (after *in situ* reduction at 400 °C) after the reaction temperature is stable. Results show that Pt/deAl-Beta displays relatively 'clean' surface, with only the appearance of adsorption bands of toluene, maleic anhydride and benzyl alcohol during the reaction due to the relatively low conversion at this temperature (Figure 6c). However, benzoate and benzyl alcohol gradually accumulated

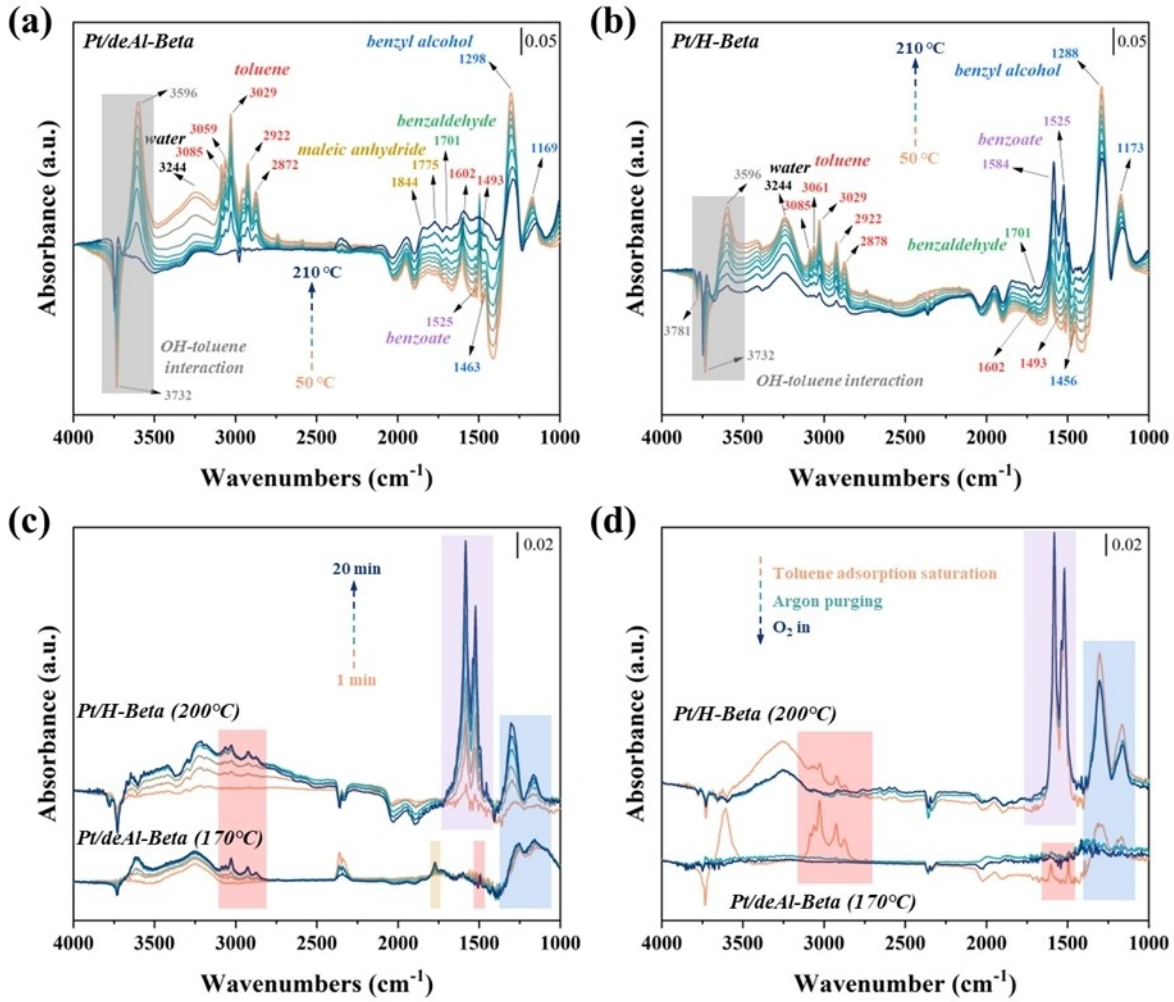

Figure 6. *In situ* DRIFTS characterisation of toluene adsorption/oxidation on Pt/deAl-Beta and Pt/H-Beta: (a, b) temperature ramping experiments (from 50 to 210 °C at 10 °C/min; 500 ppm toluene + 20 vol.% O_2 + Ar balance), (c) time-resolved experiments (at 170 °C for Pt/deAl-Beta and 200 °C for Pt/H-Beta; 500 ppm toluene + 20 vol.% O_2 + Ar balance), and (d) O_2 titration experiments (at 170 °C for Pt/deAl-Beta and 200 °C for Pt/H-Beta; toluene adsorption using 500 ppm toluene + Ar balance, pure Ar purge, and oxidation in 20 vol.% O_2 + Ar balance). The total gas flowrate for all experiments was constant at 60 mL/min.

on Pt/H-Beta with an increase in reaction time, which could lead to coking.

In situ DRIFTS of the two catalysts at different gas atmospheres was performed to study oxidation of surface-adsorbed toluene (i.e., O_2 titration, Figure 6d). During the experiments, the two catalysts were saturated first using toluene (with Ar balance, at the temperatures same to that in the time-resolved *in situ* DRIFTS, Figure 6c), then purged using Ar (to remove the weakly adsorbed species). After the Ar purge, O_2 was introduced to the system to initiate the reactions with surface adsorbed species. On Pt/deAl-Beta, only the adsorption bands of toluene and benzyl alcohol were identified at 170 °C, which could be removed by Ar purging at the same temperature. Same phenomenon was observed in the Pt/H-Beta system as well. It is worth noting that, at 200 °C in the system employing Pt/H-Beta, bands at 1522 and 1584 cm^{-1} (i.e., benzyl alcohol and benzoate) developed significantly, and the introduction of O_2 could not consume them, suggesting that these species were not on the Pt surface, and coking on Pt/H-Beta were likely related to the interaction between toluene and acid sites of H-Beta.

To get more insights into the interaction between toluene and the Pt species, the catalysts were poisoned using CO first (i.e., CO saturation followed by Ar purging for 10 min at 170 °C), then toluene was fed into the systems and DRIFTS was performed. Results (Figure 7a) show that both Pt/deAl-Beta and Pt/H-Beta display a CO adsorption band at 2058 cm^{-1} after the weakly adsorbed CO was removed by Ar purge, and the band changed as a function of time after introducing toluene. To quantify the process of toluene replacing CO on the Pt surfaces, the CO adsorption intensity was normalised by that at time zero (t = 0 min in Pt/deAl-Beta). Figure 7b presents the relative intensity normalised using the CO adsorption band intensity of Pt/deAl-Beta (at t = 0 min), showing that Pt/deAl-Beta has intrinsically higher CO absorption capacity than Pt/H-Beta, and hence more accessible Pt surface. After the introduction of toluene to the two systems, the CO on the Pt surface of Pt/deAl-Beta could be replaced almost completely by toluene

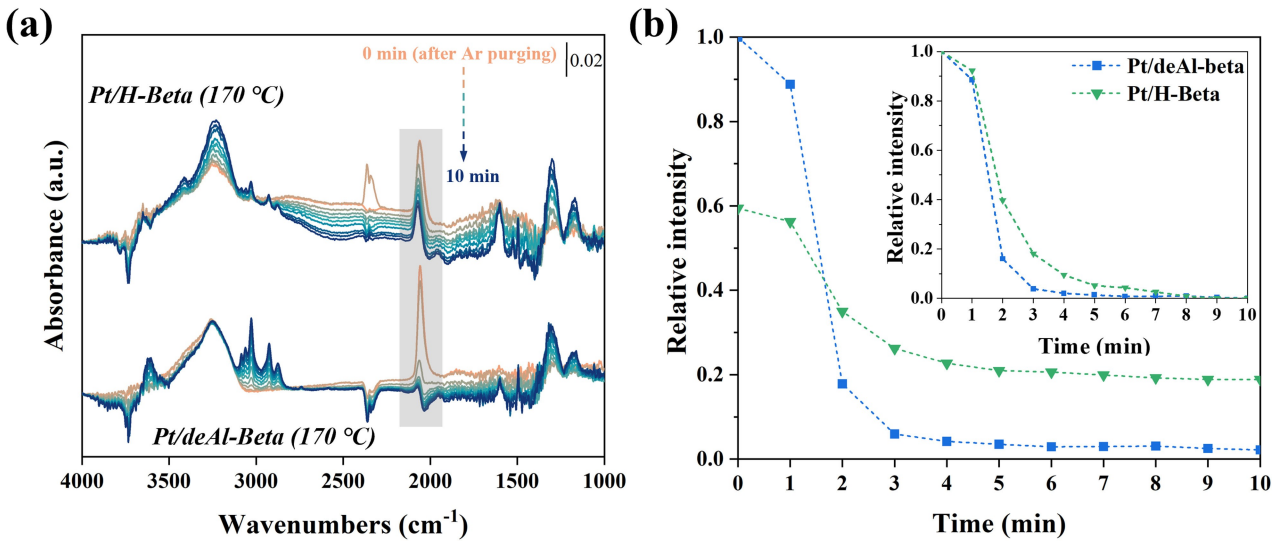

Figure 7. *In situ* DRIFTS studies of toluene-catalyst interaction over Pt/deAl-Beta and Pt/H-Beta at 170 °C: (a) time-resolved DRIFTS spectra of toluene replacing the adsorbed CO on Pt surface (the catalysts were pre-saturated using Ar-balanced 2 vol.% CO, then purged using pure Ar, followed by introducing Ar-balanced 500 ppm toluene; the total flowrate is kept constant at 60 mL/min); (b) quantitative analysis of the adsorbed CO on the Pt surfaces amount (insert: rate of CO replacement by toluene).

(nearly 98%), whilst it was only ~68% for Pt/H-Beta. The inset of Figure 7b shows the rates of toluene replacing the surface CO, which was obtained by stretching the relative intensities curves in Figure 7b through treating their initial and final intensity as 1 and 0. One can see that the surface-adsorbed CO on Pt/deAl-Beta was replaced faster than that on Pt/H-Beta (note that this comparison was based only on the replaceable CO rather than all the adsorbed CO), suggesting that the Pt species of Pt/deAl-Beta could interact with toluene easily and strongly, which agrees with the findings of toluene-TPD and NMR relaxation. Accordingly, based on the findings and discussion above, we speculate that the deAl-Beta support here played an important role in stabilising good 'quality' of Pt species via the hydroxyl groups (such as silanol nest and isolated internal Si-OH) to interact with toluene and convert it under oxidising conditions. Conversely, for H-Beta, due to the presence of Al species in it, the resulting Pt species are less effective for catalytic oxidation reactions, and the acidity of the support also cause coking.

Conclusions

Catalyst carriers/supports are other important aspects of making effective catalysts. This work employed different Beta zeolites (as the supports) to prepare the supported Pt catalysts for catalytic oxidation reactions (toluene as the model compound) and explored the effect of the supports on the properties of the Pt phases and their activity in the catalysis. Comprehensive characterisation of the resulting catalysts was conducted to know the nature of the catalysts (such as Pt nanoparticle size, dispersion, oxidation state, electronic and coordination structure) and establish the correlation between the property of the zeolite supports and that of the resulting Pt phases. We found that dealumination of H-Beta is necessary to make the Al-free Beta (i.e., deAl-Beta), in which the abundant hydroxyl groups (such as silanol nest and isolated internal Si-OH) are highly beneficial to stabilise the Pt precursor and form active Pt-O species (i.e., the Pt/deAl-Beta catalyst) for the oxidation catalysis, whilst the H-Beta support anchors Pt species *via* the interactions between the Pt precursor and Al-OH and isolated external Si-OH, leading to the formation of less active metallic Pt nanoparticles (after reduction, i.e., the Pt/H-Beta catalyst). Comparative *in situ* DRIFTS characterisations of the reaction systems employing different catalysts revealed key surface intermediates and substrate-catalyst interactions. In detail, Pt/deAl-Beta showed high toluene adsorption ability and strong interaction with toluene, enabling partially oxidation of the adsorbed toluene to benzyl alcohol facilitated by the domestic hydroxyl groups on the deAl-Beta zeolite, which could be promptly converted into the subsequent oxidised intermediates such as benzaldehyde, benzoate and maleic acid and eventually the product CO_2. Conversely on Pt/H-Beta, although similar reaction intermediates were identified, the catalyst was prone to accumulate oxidised intermediates ascribing to the acid-rich feature of the H-Beta support. Findings of the work are expected to provide guidance on the design and optimisation of zeolite-supported metal catalysts by engineering the hydroxyl groups in the zeolitic carriers for effective catalysis in different applications.

Experimental Section

Catalyst Preparation

Dealumination of zeolite Beta (**deAl-Beta**) was achieved by treating 2 g of the **H-Beta** (obtained by calcination of the parent NH_4-Beta at 550 °C for 5 h) using 40 mL HNO_3 solution (13 mol/L) at 100 °C for 24 h under magnetic stirring (350 rpm).[53] After the acid treatment,

the resulting sample was washed with deionised water and separated by centrifugation until the pH value of supernatant was around 7–8, and then dried at 100 °C in an oven overnight. To prepare the control with less silanol nest (i.e., **calcinated deAl-Beta**), deAl-Beta was calcinated at 550 °C for 6 h.[54] Information on materials and chemicals are detailed in the Electric Supplementary Information (ESI). The Pt catalysts were prepared by impregnation. Typically, 0.4 g zeolite support (including H-Beta (silicon to alumina molar ratio, SAR = 12), **high silica H-Beta** (SAR = 150), deAl-Beta and calcinated deAl-Beta was dispersed in ~20 mL $Pt(NH_3)_4(NO_3)_2$ aqueous solution and stirred for 16 h at room temperature. Then, the solution was evaporated at 85 °C overnight, and the resulting powder was dried in an oven at 120 °C. The resulting catalysts were denoted as **Pt/H-Beta, Pt/H-Beta 150, Pt/deAl-Beta and Pt/calcinated deAl-Beta**. Details of the characterization techniques for assessing the physicochemical properties of zeolites and catalysts are provided in the ESI.

Evaluation of catalytic performance

Catalytic toluene oxidation over the Pt catalysts under investigation was conducted using a fixed-bed flow reactor with a quartz tube (inner diameter of 4 mm) at atmospheric pressure. Before reaction, the catalysts were reduced at 400 °C (for 1 h, heating rate of 5 °C/min) in a tube furnace using pure H_2 (at 50 mL/min). In a typical experiment, ~0.05 g catalyst (pelletized, 355–500 μm) was placed between quartz wool plugs in the reactor, then the gases were introduced to the reactor (via mass flow controllers for the catalysis, giving a total flowrate of 160 mL/min consisting of 20 vol.% O_2 and Ar balance). Toluene (500 ppm) and water vapour (4.5 vol.%) were introduced by passing the carrier gas (Ar) through saturators (for toluene, the saturator was placed in an ice/water bath; for water vapor, the saturator was placed in a thermostatic bath at 60 °C). The gas line after the water saturator was heated to prevent condensation. K-type thermocouple was placed in the centre of the catalyst bed to monitor the bed temperature, and the outlet steam of the reaction system was analysed online using mass spectrometer (Hiden Analytical HPR 20).

Acknowledgements

This project has received funding from the European Union's Horizon 2020 research and innovation program under grant agreement No 872102. R.Z. thanks the China Scholarship Council (CSC, file no. 201906740020) and The University of Manchester for the joint PhD studentship to support his research. C.D. and X.F. would also like to acknowledge the EPSRC, grant no. EP/V026089/1, for supporting the research. We are also grateful to Diamond Light Source for access to beamline B18 for the *ex situ* XAFS measurements.

Conflict of Interests

The authors declare no conflict of interest.

Data Availability Statement

The data that support the findings of this study are available from the corresponding author upon reasonable request.

Keywords: Beta zeolite · Pt nanoparticles · dealumination · hydroxyl groups · toluene oxidation

[1] L. Zhu, D. Shen, K. H. Luo *J. Hazard. Mater.* **2020**, *389*, 122102.
[2] D. Murindababisha, A. Yusuf, Y. Sun, C. Wang, Y. Ren, J. Lv, H. Xiao, G. Z. Chen, J. He, *Environ. Sci. Pollut. Res. Int.* **2021**, *28*, 62030–62060.
[3] K.-H. Kim, J. E. Szulejko, N. Raza, V. Kumar, K. Vikrant, D. C. W. Tsang, N. S. Bolan, Y. S. Ok, A. Khan, *J. Cleaner Prod.* **2019**, *241*, 118408.
[4] M. S. Kamal, S. A. Razzak, M. M. Hossain, *Atmos. Environ.* **2016**, *140*, 117–134.
[5] L. F. Liotta, *Appl. Catal. B* **2010**, *100*, 403–412.
[6] T. Gan, X. Chu, H. Qi, W. Zhang, Y. Zou, W. Yan, G. Liu, *Appl. Catal. B* **2019**, *257*, 117943.
[7] Y. T. Lai, T. C. Chen, Y. K. Lan, B. S. Chen, J. H. You, C. M. Yang, N. C. Lai, J. H. Wu, C. S. Chen, *ACS Catal.* **2014**, *4*, 3824–3836.
[8] R. Peng, X. Sun, S. Li, L. Chen, M. Fu, J. Wu, D. Ye, *Chem. Eng. J.* **2016**, *306*, 1234–1246.
[9] J. Zhang, X. Xu, S. Zhao, X. Meng, F.-S. Xiao, *Catal. Today* **2023**, *410*, 56–67.
[10] J. Wang, Y. Shi, F. Kong, R. Zhou, *Journal of Environmental Sciences* **2023**, *124*, 505–512.
[11] M.-R. Kim, S. Kim, *Catalysts* **2022**, *12*, 622.
[12] R. El Khawaja, S. Sonar, T. Barakat, N. Heymans, B.-L. Su, A. Löfberg, J.-F. Lamonier, J.-M. Giraudon, G. De Weireld, C. Poupin, R. Cousin, S. Siffert, *Catal. Today* **2022**, *405–406*, 212–220.
[13] J. Zhang, C. Rao, H. Peng, C. Peng, L. Zhang, X. Xu, W. Liu, Z. Wang, N. Zhang, X. Wang, *Chem. Eng. J.* **2018**, *334*, 10–18.
[14] C. Chen, J. Zhu, F. Chen, X. Meng, X. Zheng, X. Gao, F.-S. Xiao, *Appl. Catal. B* **2013**, *140–141*, 199–205.
[15] C. Chen, Q. Wu, F. Chen, L. Zhang, S. Pan, C. Bian, X. Zheng, X. Meng, F.-S. Xiao, *J. Mater. Chem. A* **2015**, *3*, 5556–5562.
[16] P. H. Ho, J. Woo, R. F. Ilmasani, M. A. Salam, D. Creaser, L. Olsson, *ACS Engineering Au* **2021**, *2*, 27–45.
[17] I. Friberg, N. Sadokhina, L. Olsson, *Appl. Catal. B* **2019**, *250*, 117–131.
[18] M.-C. Silaghi, C. Chizallet, P. Raybaud, *Microporous Mesoporous Mater.* **2014**, *191*, 82–96.
[19] R. Zhang, R. Zou, W. Li, Y. Chang, X. Fan, *Microporous Mesoporous Mater.* **2022**, *333*, 111736.
[20] C. Chen, S. Zhang, Z. Wang, Z.-Y. Yuan, *J. Catal.* **2020**, *383*, 77–87.
[21] C. Chen, M. Sun, Z. Hu, Y. Liu, S. Zhang, Z.-Y. Yuan, *Chin. J. Catal.* **2020**, *41*, 276–285.
[22] D. Yu, W. Dai, G. Wu, N. Guan, L. Li, *Chin. J. Catal.* **2019**, *40*, 1375–1384.
[23] W. Gac, W. Zawadzki, G. Słowik, M. Kuśmierz, S. Dzwigaj, *Appl. Surf. Sci.* **2021**, *564*, 150421.
[24] D. Zhao, X. Tian, D. E. Doronkin, S. Han, V. A. Kondratenko, J. D. Grunwaldt, A. Perechodjuk, T. H. Vuong, J. Rabeah, R. Eckelt, U. Rodemerck, D. Linke, G. Jiang, H. Jiao, E. V. Kondratenko, *Nature* **2021**, *599*, 234–238.
[25] R. Ryoo, J. Kim, C. Jo, S. W. Han, J.-C. Kim, H. Park, J. Han, H. S. Shin, J. W. Shin, *Nature* **2020**, *585*, 221–224.
[26] A. Rokicińska, M. Drozdek, B. Dudek, B. Gil, P. Michorczyk, D. Brouri, S. Dzwigaj, P. Kuśtrowski, *Appl. Catal. B* **2017**, *212*, 59–67.
[27] A. Rokicińska, P. Majerska, M. Drozdek, S. Jarczewski, L. Valentin, J. Chen, A. Slabon, S. Dzwigaj, P. Kuśtrowski, *Appl. Surf. Sci.* **2021**, *546*, 149148.
[28] I. Friberg, A. H. Clark, P. H. Ho, N. Sadokhina, G. J. Smales, J. Woo, X. Auvray, D. Ferri, M. Nachtegaal, O. Kröcher, L. Olsson, *Catal. Today* **2021**, *382*, 3–12.
[29] H. Jiang, Z. Liu, C. Yao, S. Wang, *Microporous Mesoporous Mater.* **2022**, *335*, 111842.
[30] S. K. Matam, E. V. Kondratenko, M. H. Aguirre, P. Hug, D. Rentsch, A. Winkler, A. Weidenkaff, D. Ferri, *Appl. Catal. B* **2013**, *129*, 214–224.
[31] J. Zhang, M. Cheng, Y. Jiao, L. Wang, J. Wang, Y. Chen, X. Li, *Appl. Surf. Sci.* **2021**, *559*, 149950.
[32] F. Yi, H. Chen, L. Huang, C. Hu, J. Wang, T. Li, H. Wang, Z. Tao, Y. Yang, Y. Li, *Fuel* **2021**, *300*, 120694.
[33] F. Yi, Y. Chen, Z. Tao, C. Hu, X. Yi, A. Zheng, X. Wen, Y. Yun, Y. Yang, Y. Li, *J. Catal.* **2019**, *380*, 204–214.
[34] P. S. F. Mendes, A.-L. Taleb, A.-S. Gay, A. Daudin, C. Bouchy, J. M. Silva, M. F. Ribeiro, *J. Mater. Chem. A* **2017**, *5*, 16822–16833.
[35] C. Chen, F. Chen, L. Zhang, S. Pan, C. Bian, X. Zheng, X. Meng, F.-S. Xiao, *Chem. Commun.* **2015**, *51*, 5936–5938.
[36] J. Kim, E. E. Kwon, J. E. Lee, S. H. Jang, J. K. Jeon, J. Song, Y. K. Park, *J. Hazard. Mater.* **2021**, *403*, 123934.

[37] C. D'Agostino, P. Bräuer, J. Zheng, N. Robinson, A. P. E. York, L. Song, X. Fan, *Materials Today Chemistry* **2023**, *29*, 101433.
[38] C. D'Agostino, A. P. E. York, P. Bräuer, *Materials Today Chemistry* **2022**, *24*, 100901.
[39] N. Robinson, P. Brauer, A. P. E. York, C. D'Agostino, *Phys. Chem. Chem. Phys.* **2021**, *23*, 17752–17760.
[40] A. Lu, H. Sun, N. Zhang, L. Che, S. Shan, J. Luo, J. Zheng, L. Yang, D.-L. Peng, C.-J. Zhong, B. Chen, *ACS Catal.* **2019**, *9*, 7431–7442.
[41] J. Li, H. Na, X. Zeng, T. Zhu, Z. Liu, *Appl. Surf. Sci.* **2014**, *311*, 690–696.
[42] J. Fan, Y. Sun, M. Fu, J. Li, D. Ye, *J. Hazard. Mater.* **2022**, *424*, 127505.
[43] Y. Du, G. Xiao, Z. Guo, B. Lin, M. Fu, D. Ye, Y. Hu, *Sci. Total Environ.* **2022**, *833*, 155288.
[44] G. Hou, T. Fu, X. Li, Q. Ma, Z. Li, *Appl. Catal. A* **2022**, *642*, 118713.
[45] J. Chen, Y. Yang, S. Zhao, F. Bi, L. Song, N. Liu, J. Xu, Y. Wang, X. Zhang, *ACS Catal.* **2022**, *12*, 8069–8081.
[46] Z. Wang, P. Ma, K. Zheng, C. Wang, Y. Liu, H. Dai, C. Wang, H.-C. Hsi, J. Deng, *Appl. Catal. B* **2020**, *274*, 118963.
[47] Z. Wang, S. Xie, Y. Feng, P. Ma, K. Zheng, E. Duan, Y. Liu, H. Dai, J. Deng, *Appl. Catal. B* **2021**, *298*, 120612.
[48] J. Liu, L. Zeng, X. Xu, J. Xu, X. Fang, Y. Bian, X. Wang, *Phys. Chem. Chem. Phys.* **2022**, *24*, 14209–14218.
[49] C. Zhang, C. Wang, H. Huang, K. Zeng, Z. Wang, H.-p. Jia, X. Li, *Appl. Surf. Sci.* **2019**, *486*, 108–120.
[50] H. Sun, Z. Liu, S. Chen, X. Quan, *Chem. Eng. J.* **2015**, *270*, 58–65.
[51] L. Zhao, Z. Zhang, Y. Li, X. Leng, T. Zhang, F. Yuan, X. Niu, Y. Zhu, *Appl. Catal. B* **2019**, *245*, 502–512.
[52] A. P. Antunes, M. F. Ribeiro, J. M. Silva, F. R. Ribeiro, P. Magnoux, M. Guisnet, *Appl. Catal. B* **2001**, *33*, 149–164.
[53] C. Hammond, S. Conrad, I. Hermans, *Angew. Chem. Int. Ed. Engl.* **2012**, *51*, 11736–11739.
[54] I. C. Medeiros-Costa, E. Dib, N. Nesterenko, J. P. Dath, J. P. Gilson, S. Mintova *Chem. Soc. Rev.* **2021**, *50*, 11156–11179.

Manuscript received: June 29, 2023
Revised manuscript received: September 14, 2023
Accepted manuscript online: September 20, 2023
Version of record online: October 25, 2023